Iron and Steel Industry Emissions: A Global Analysis of Trends and Drivers

Jinjian Zhang[1,2], Huizhong Shen[1,2,*], Yilin Chen[1,2,3], Jing Meng[4], Jin Li[5], Jinling He[1,2], Peng Guo[1,2], Rong Dai[5], Yuanzheng Zhang[5], Ruibin Xu[1,2], Jinghang Wang[5], Shuxiu Zheng[5], Tianyang Lei[6], Guofeng Shen[5], Chen Wang[1,2], Jianhuai Ye[1,2], Lei Zhu[1,2], Haitong Zhe Sun[7], Tzung-May Fu[1,2], Xin Yang[1,2], Dabo Guan[6], Shu Tao[1,2,5,8]

[1] Guangdong Provincial Observation and Research Station for Coastal Atmosphere and Climate of the Greater Bay Area, School of Environmental Science and Engineering, Southern University of Science and Technology, Shenzhen 518055, China

[2] Shenzhen Key Laboratory of Precision Measurement and Early Warning Technology for Urban Environmental Health Risks, School of Environmental Science and Engineering, Southern University of Science and Technology, Shenzhen 518055, China

[3] School of Urban Planning and Design, Peking University, Shenzhen Graduate School, Shenzhen 518055, China

[4] The Bartlett School of Sustainable Construction, University College London, London WC1E 7HB, United Kingdom

[5] College of Urban and Environmental Sciences, Peking University, Beijing 100871, China

[6] Department of Earth System Sciences, Tsinghua University, Beijing 100080, China

[7] Centre for Atmospheric Science, Yusuf Hamied Department of Chemistry, University of Cambridge, Cambridge CB2 1 EW, United Kingdom

[8] Institute of Carbon Neutrality, Peking University, Beijing 100871, China

*Corresponding author, e-mail: shenhz@sustech.edu.cn

Abstract

The iron and steel industry (ISI) is important for socio-economic progress but emits greenhouse gases and air pollutants detrimental to climate and human health. Understanding its historical emission trends and drivers is crucial for future warming and pollution interventions. Here we offer an exhaustive analysis of global ISI emissions over the past sixty years, forecasting up to 2050. We evaluate emissions of carbon dioxide and conventional and unconventional air pollutants, including heavy metals and polychlorinated dibenzodioxins and dibenzofurans. Based on this newly established inventory, we dissect the determinants of past emission trends and future trajectories. Results show varied trends of different pollutants. Specifically, $PM_{2.5}$ emissions decreased consistently during the period 1970 to 2000, attributed to adoption of advanced production technologies. Conversely, NO_x and SO_2 began declining recently due to stringent controls in major contributors like China, a trend expected to persist. Currently, end-of-pipe abatement technologies are key to $PM_{2.5}$ reduction, whereas process modifications are central for CO_2 mitigation. Projections suggest that by 2050, developing nations (excluding China) will contribute 52–54% of global ISI $PM_{2.5}$ emissions, a rise from 29% in 2019. Long-term emission curtailment will necessitate the innovation and widespread adoption of new production and abatement technologies in emerging economies worldwide.

Keywords: iron and steel industry, emission inventory, historical trends, driving forces, greenhouse gases, air pollutants

Synopsis: The assessment of emissions originating from global iron and steel industry over the long term reveals the important roles of enhanced removal efficiency and production process transitions in shaping the historical and future trajectories of greenhouse gases and air pollutant emissions.

Graphics for Manuscript

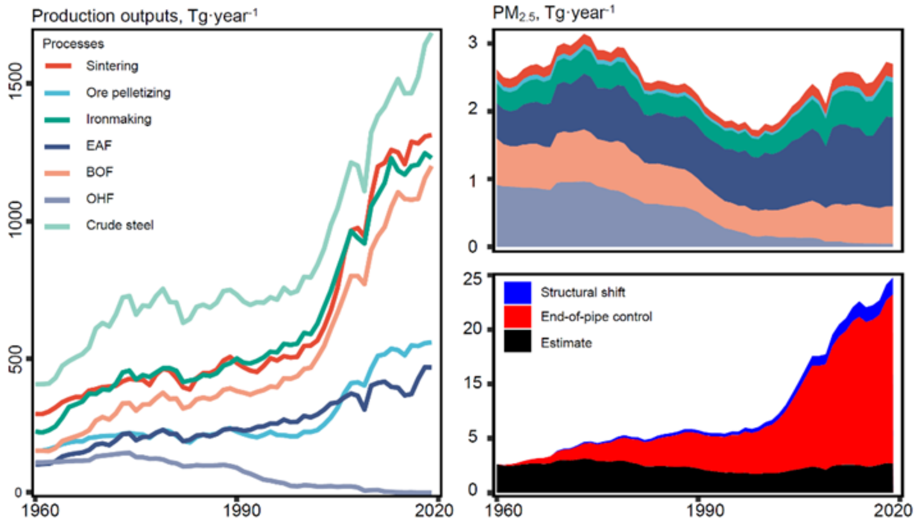

1. Introduction

The iron and steel industry (ISI) plays a pivotal role in defining modern civilization.[1] This energy- and pollution-intensive manufacturing sector account for approximately 8% of global final energy consumption and contributes 7–10% of energy-related CO_2 emissions, surpassing all other heavy industries in this regard.[2–5] Additionally, it releases various pollutants into the atmosphere, including SO_2, NO_x, CO, and particulate matter (PM).[6–9] Notably, in China, ISI emissions of dust, SO_2, and NO_x constitute 27%, 20%, and 8% respectively of the overall emissions from key manufacturing industries.[10] Recently, there has been growing concern regarding heavy metals and polychlorinated dibenzo-p-dioxins and dibenzofurans (PCDD/Fs) due to the substantial increase in global ISI production.[7,11–16] For instance, ISI is the primary stationary industrial source of PCDD/Fs in Canada and the second highest in Europe, after electricity generation.[17] In summary, the emissions from ISI are environmental issues of global significance.[18]

On a regional-to-global scale, the magnitudes of emissions from ISI are primarily determined by ISI production outputs and emission abatement measures.[19] Over the past six decades, global crude steel output has experienced significant growth, increasing from 347 Mt in 1960 to 1,879 Mt in 2020.[20] China has held the position of the largest producer and consumer of iron and steel since 1996,[10] with India and Africa assuming increasingly prominent roles in this industry.[21,22] Consequently, the rapid expansion of production has resulted in substantial increases in air pollutant emissions from China and other emerging economies.[6,23–25] Simultaneously, the implementation of environmental protection policies has stimulated the adoption of measures to control air pollutant emissions in the ISI, partially offsetting the rise in emissions. The global trend in ISI emissions is shaped by the interplay between expanding production and increasingly stringent emission controls. However, variations in the rate of installation of end-of-pipe abatement facilities across countries have led to divergent emission trends. Developed countries generally exhibit higher installation rates, while developing countries benefit from their "latecomer" advantage, enabling them to catch up swiftly.[26] In particular, China's recent adoption of the ultra-low emission transformation, which incorporates multiple control measures for the iron and steel industry, has significantly reduced the nation's ISI emissions.[19,27–30] As of now, the precise extent to which production and abatement factors have influenced and will continue to drive regional and global trends in ISI emissions remains unclear.

The complexity of the ISI structure poses challenges when assessing emission trends and determining their underlying drivers. The ISI comprises diverse manufacturing processes, including sintering, ore pelletizing, ironmaking, steelmaking, casting, among others.[3,31,32] These processes employ various production technologies, such as blast furnace ironmaking (BF), electric arc furnace steelmaking (EAF), basic oxygen furnace steelmaking (BOF), open hearth furnace steelmaking (OHF). Each of these processes/technologies emits a wide range of air pollutants and greenhouse gases to varying extents. The shares of these processes and technologies vary from one country to another. For instance, in the steel production process, there are two basic routes: the BF-BOF route and the EAF route (Figure S1). In 2017, these two routes accounted for 71.6% and 28.0% of the global steel production, respectively.[20] The BF-BOF route dominates in China, Japan, Russia, South Korea, and Germany, whereas the EAF route is more commonly employed in the United States, India, and Turkey.[33] Notably, BF-BOF is typically more polluting than EAF, which leads to a great diversity of emission intensities across countries.[34] Certain highly polluting technologies, such as OHF, which were prevalent in the mid-20th century, are now obsolete.[35] Conversely, cleaner technologies like direct reduction and smelting reduction processes have emerged, but their market penetration remains limited.[35] The turnover of processes and technologies in the ISI sector is expected to significantly influence global ISI emission trends, which has not been fully quantified.

In this study, we conduct an extensive assessment of global ISI emissions for multiple air pollutants, including heavy metals, PCDD/Fs, CO_2, and conventional air pollutants, based on country-specific production processes and technologies from 1960 to 2019. Distinguishing our research from preceding works, we offer an exhaustive compilation of the global long-term progression of ISI production and control technologies, which have not been comprehended previously. Additionally, we assess a wider array of air pollutants, some of which have not been globally analyzed before. By utilizing this emission inventory, we investigate the historical ISI emissions trends worldwide, with a specific focus on the primary determinants (e.g., ISI output, national environmental policies, production processes, and end-of-pipe control technologies) that have contributed to the temporal shifts in both global and regional ISI emissions.

2. Methodology

2.1 Emission estimation

The ISI processes considered in this study are sintering, ore pelletizing, ironmaking, and steelmaking (including OHF, BOF, and EAF). A simplified flow diagram of iron and steel production is shown in Figure S1. We calculate the emissions of CO_2 and air pollutants including particulate matters (distinguished by size range as $PM_{2.5}$, PM_{10}, and TSP), BC, OC, SO_2, NO_x, CO, PCDD/Fs, and 11 heavy metals (Hg, Cd, Cr, Ni, As, Pb, Cu, Mn, Se, V, and Zn). Emissions are calculated using a bottom-up approach with the following formulas:

$$E_j = \sum_{i,k} A_i \times EF_{i,j} \times R_{i,k} \times (1 - \eta_k) \quad (1)$$

where the subscripts i, j, and k denote the process and production technology, pollutant, and end-of-pipe abatement technology, respectively. E_j represents the total emission of pollutant j from all processes. A_i is the activity intensity of process i (e.g., the amount of pig iron sintered or steel produced). The variable $EF_{i,j}$ represents the uncontrolled emission factor (*EF*, defined as the amount of pollutant emitted per unit level of activity conducted) of pollutant j for process i, while $R_{i,k}$ represents the proportion of end-of-pipe abatement technology k adopted in process i. Finally, η_k represents the removal efficiency of end-of-pipe abatement technology k.

2.2 Activity data and emission factors

The process-specified activity data in this study are derived from the Steel Statistical

Yearbook by the World Steel Association and the PKU-FUEL database.[36,37] To elaborate further, the data regarding ironmaking (outputs of pig iron) and steelmaking production (outputs of OHF, BOF, and EAF) primarily rely on the statistics available in the Steel Statistical Yearbook. In instances where data gaps or missing information are encountered, we supplement these areas using data extracted from the PKU-FUEL database. For the estimation of sintering and ore pelleting outputs, we base our calculations on the production statistics related to iron ore and incorporate export and import data of iron ore according to Steel Statistical Yearbook after 1978, including iron ore exports from Brazil, India, Australia, South Africa, and Canada, as well as iron ore imports from China, Japan, South Korea, Germany, France, Italy, and the United Kingdom.[38] These countries account for 60-80% of the world's total iron ore imports and exports.[36] The iron ore import and export data of these countries before 1978 were obtained based on linear extrapolation. Previous studies have shown that *EF* is a major source of uncertainty when compiling emission inventories.[39,40] To reduce this uncertainty, we collect as many *EF*s as possible for individual pollutants, processes, and technologies, and used Monte Carlo simulations to determine the distributions of *EF*s and calculate the uncertainty in emissions caused by *EF*s. The technology splitting method is used to simulate the changes in the division of different end-of-pipe abatement facilities over time by country (Text S1).[39,41,42] A total of 225 countries and regions are included and classified into four categories: (1) the United States, (2) other developed countries (43 countries), (3) China, and (4) other developing countries (180 countries). In the analysis that follows, we separate China from the developing country category. For each country category, the utilization ratios of end-of-pipe abatement facilities are either derived from the literature or calculated using an S-shaped regression model.[6,41,42] For China, ultra-low emission transformation has strict emission standards, which are often achieved by combining various treatment facilities. We treat this as one treatment facility in our calculation and determine its η according to the study of Zhu et al.[27] At the same time, considering the various environmental protection policies issued by China in recent years,[43] we separately adjust the proportions of abatement facilities for China in 2010-2019. The η values of various abatement facilities and pollutants are listed in Table S1. The η values for BC and OC are adopted from those of $PM_{2.5}$. The η values for CO, CO_2, and PCDD/Fs are set to 0 for all abatement facilities. For heavy metals, we employ the *EF*s reported by Wang et al.,[6] which considered smelting processes and more effective flue gas pollution control devices by year.

It is worth noting that the emission of CO is significantly affected by the gas-recycling ratio.[44] We collect the historical information and fit the curve of the gas-recycling ratio for BOF and BF with a logistic growth model in China, and calculate the *EF*s of CO following Streets et al.[45] The details are provided in Table S2 and Figure S2. The United States and other developed countries typically have high gas-recycling ratios, while developing countries may vary greatly. For these country categories, we borrow *EF*s of CO from previous studies.[40,46] The *EF*s of various species and processes used in this study are summarized in Table S3 and S4. The parameters used to calculate the proportions of end-of-pipe abatement technologies for different country categories are listed in Table S5 and S6.

2.4 Future scenario projections

To investigate the effects of changing the process structure and removal efficiency on emissions, we design different scenarios to project the future trends. The projection of the ISI production output is based on the International Energy Agency,[3] which shows a continuing increase in the near future. Based on the projected production output, we design the following three scenarios: 1) stable and slow (SS), 2) strict policies (SP), and 3) radical policies (RP). In the SS scenario, we assume that the industry structure will not change and that removal efficiency will continue to improve in response to existing policies. In the SP scenario, strict policies will lead to the adoption of more efficient removal devices, and EAFs will gradually replace BOFs with a decrease in the demand for pig iron. In the RP scenario, radical environmental protection policies will be implemented, leading to further improvements in removal efficiency, and sintering and pelletizing in developed countries will rely more on imports. The key parameters of the three scenarios are summarized in Table S7.

2.5 Uncertainty analysis

Monte Carlo simulations are used to evaluate the uncertainty in the emission estimates and future scenario projections. We randomly sample from given distributions and calculate the results 10,000 times. Based on previous studies,[40,42,47–49] we assume that the activity data of various ISI processes followed a uniform distribution with a ±10% variation intervals around the means, and that the collected *EF*s followed a lognormal distribution, as shown in Table S3. We used Cox's method to construct the confidence interval for the expected values of *EF*s based on the different numbers of *EF*s collected for each process.[50] The detailed formula can be found in our previous study.[47] Throughout the main text, emission estimates are presented as medians and interquartile ranges.

3. Results and discussion

3.1 Annual emissions and source profiles

In 2019, the global emission of $PM_{2.5}$ from ISI was 2.70 Tg, and the emissions of SO_2, NO_x, and CO_2 were 0.88 Tg, 0.57 Tg, and 2,548 Tg, respectively (Table 1). The global estimates for other pollutants are listed in Table 1. Emissions for individual countries are provided in Tables S8. Our estimate of $PM_{2.5}$ emissions for 2007 (2.40 Tg) is similar to the estimate by Huang et al. (2.81 Tg) for the same year.[39] However, there are significant differences when comparing our study with two other global emission inventories, the Community Emissions Data System (CEDS) and Emission Database for Global Atmospheric Research (EDGAR v6.1).[51,52] The ISI emissions of SO_2 and NO_x reported by CEDS are 66–263% and 238–457% higher than our study, likely due to differences in the treatments of *EF*s and end-of-pipe abatement. The estimates of SO_2, NO_x, and $PM_{2.5}$ by EDGAR v6.1 are substantially lower than our estimates (by 99.35%–99.92%, 95.89%–99.50%, 89.24%–93.3%, respectively), which may be due to mismatched source categorization. Lower estimates for ISI emissions by EDGAR were also reported previously.[19] We also compared the emissions of these global inventories with authoritative regional inventories. Our estimate of $PM_{2.5}$ emissions from China's ISI is closer to the results of the Multi-resolution Emission Inventory for China (MEIC v1.3) than EDGAR v6.1 (Figure S3). Note that CEDS scaled its default estimates to match existing authoritative country-level inventories, including NEI, EMEP, MEIC, etc.[52,53] Therefore, emissions between CEDS and these inventories are expected to be identical. The disparities between inventories often stem from differences in source classification commonly found among various emission inventories. For example, EDGAR classified the fuel combustion of ISI in the Manufacturing Industries and Construction sector, but we treat it as ISI emissions along with the emissions from production processes.[51] The selection of activity data, EFs, and control devices further contributed to the divergences between inventories. We cannot further justify which global inventory is more accurate due to the lack of detailed compilation information, but the differences between inventories highlight the uncertainty in ISI emission estimates. Our estimates, which include updated EFs and time- and region-specific production and abatement technology divisions, are expected to better capture the spatiotemporal variations in ISI emissions for the globe and for individual countries. This allows us to assess and compare the factors driving ISI emissions across countries (see subsequent sections).

Table 1. Global emissions of various pollutants from the iron and steel industry in 2019. The units are kg I-TEQ·year^{-1} for PCDD/Fs and Tg·year^{-1} for all others.

Pollutant	Emission	Interquartile range	Pollutant	Emission	Interquartile range
$PM_{2.5}$	2.70	2.33–3.18	SO_2	0.88	0.75–1.04
PM_{10}	4.10	3.53–4.84	NO_x	0.57	0.47–0.69
TSP	5.48	4.75–6.43	CO	67.9	58.7–79.4
BC	0.16	0.12–0.21	Heavy metals	0.04	0.03–0.05
OC	0.51	0.46–0.58	CO_2	2,548	2,400–2,713
PCDD/Fs	9.82	7.00–14.0			

We find that the source profiles of different species vary widely, as shown in Figure 1. Sintering is an important contributor to ISI emissions. During sintering, pollutants in the raw materials are released through the thermal metallurgy process as flue gas,[7,54] making it the largest source of SO_2 (79%), NO_x (74%), CO (47%), PCDD/Fs (74%), Cu (38%), and Se (54%) among all ISI processes. Previous studies have also reported similar high contributions of sintering to ISI emissions.[54–56] The primary emission source of PM is the steelmaking process (EAF+BOF+OHF), accounting for 71% of the total $PM_{2.5}$ from ISI (60% of TSP and 69% of PM_{10}). For PM components (i.e., BC, OC, and heavy metals), BC mainly comes from the ironmaking process (contributing 98% of BC), which involves coke combustion for iron ore melting. BOF is the main source of OC, As, and Pb, accounting for 86%, 87%, and 72%, respectively. EAF, which uses recycled scrap steel, is the main sources of Cd, Cr, Hg, Ni, Mn, and Zn, which are mostly emitted during scrap melting.[57,58] Ironmaking and sintering account for 80% and 13% of the CO_2 emission from ISI, respectively.

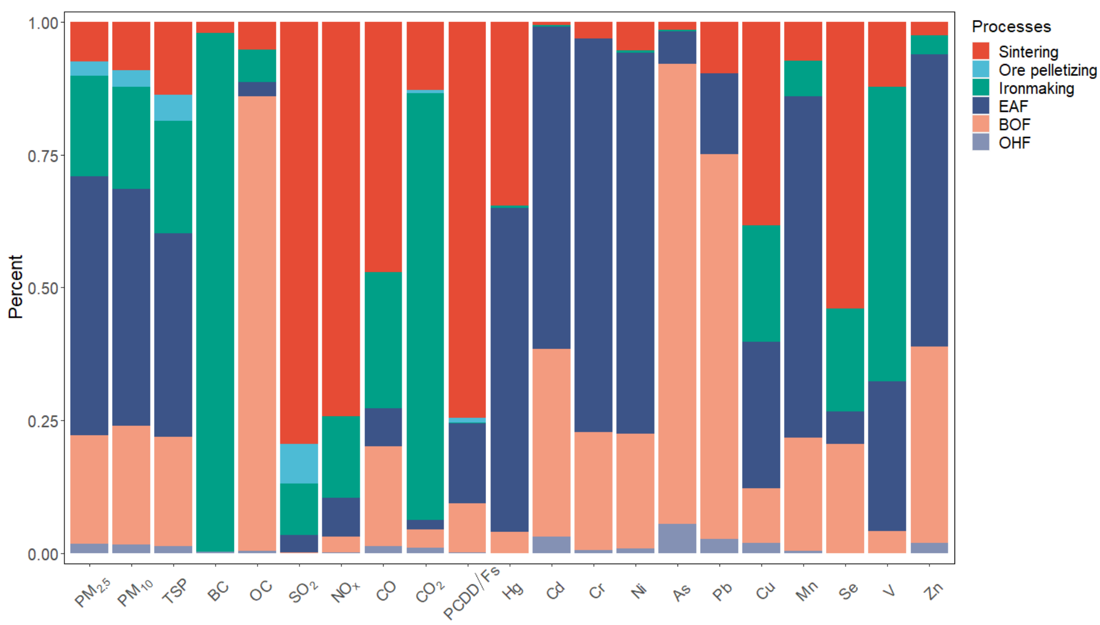

Figure 1. The contributions of different processes to the pollutant emissions from of the iron and steel industry in 2019.

3.2 Spatial distributions at the national scale

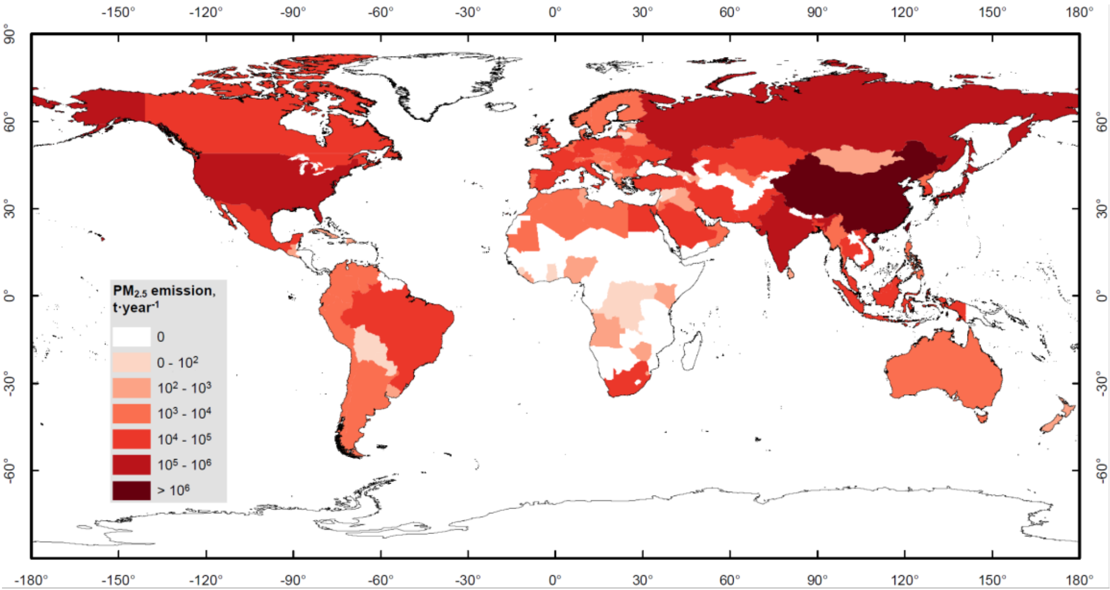

Figure 2. Annual $PM_{2.5}$ emissions from the iron and steel industry in 2019 by country. The world shapefiles were obtained from Standard Map Services of the Ministry of Natural Resources of the People's Republic of China (http://bzdt.ch.mnr.gov.cn/browse.html?picId=%224o28b0625501ad13015501ad2bfc0074%22).

The significant differences among countries lead to a tremendous spatial imbalance in global ISI emissions (Figure 2 and Table S8). East Asia, South & Southeast Asia, and Europe are three hotspots for ISI emissions. South & Southeast Asia emitted 30% of the global SO_2 emission from ISI, while East Asia and Europe emitted 27% and 23%, respectively. East Asia has the largest emissions of $PM_{2.5}$ (46%), NO_x (59%), PCDD/Fs (66%), and CO_2 (64%). For individual countries, China emitted more than 50% of the global ISI emissions of OC (63%), CO_2 (54%), PCDD/Fs (55%), As (60%), Pb (57%), and Se (58%), followed by India. As a result of the increasing steel output in India and the significant emission reduction in China in recent years,[27,28,30] India has become the largest SO_2 emitter in 2019, accounting for 29% of the global total. Emissions of CO_2, PCDDF/s, As, Pb, Cu, Se, and V from Japan are second only to China and India, accounting for about 5–6% of the global total. The United States is also a high-emission country, where Hg, Cd, Cr, Ni, Mn, and Zn emissions accounts for 7–9% of the global total, due mainly to the adoption of EAF. Although EAF is cleaner than BF-BOF for most pollutants, it has high emission potential for heavy metals. The nine countries leading in crude steel production (i.e., China, India, the United States, Russia, Japan, South Korea, Turkey, Iran, and Ukraine) contribute more than three-quarters of the global ISI emissions of $PM_{2.5}$, SO_2, NO_x, and heavy metals.

Due to a low installation rate of abatement facilities and relatively outdated production technology, developing countries, which only produced 22% of crude steel, contributed 39% of total $PM_{2.5}$, 69% of SO_2, and 35% of NO_x. The average emission intensities of developing countries are 2.51 ton of $PM_{2.5}$, 1.44 ton of SO_2, and 0.47 ton of NO_x per thousand ton of crude steel produced. On the contrary, China has recently achieved a significant reduction in ISI emissions due to strict environmental protection policies that control PM and SO_2 emissions from ISI. The emissions of $PM_{2.5}$ and SO_2 in China in 2019 show relatively low shares in the global totals (37% and 19%, respectively) compared to its large share of crude steel production (53%). The emission intensities of $PM_{2.5}$ (1.01 $t \cdot kt^{-1}$), SO_2 (0.17 $t \cdot kt^{-1}$), and NO_x (0.29 $t \cdot kt^{-1}$) are 60%, 88%, and 38% lower than those of developing countries. In the United States, the average emission intensities of SO_2 (0.03 $t \cdot kt^{-1}$) and NO_x (0.04 $t \cdot kt^{-1}$) are among the lowest due to the adoption of EAF and highly-effective emission controls. Note that EAF has a higher *EF*s of heavy metals than BOF, which leads to higher emission intensities of Hg (56 $g \cdot kt^{-1}$), Cd (112 $g \cdot kt^{-1}$), Cr (898 $g \cdot kt^{-1}$), Ni (337 $g \cdot kt^{-1}$), Mn (4,492 $g \cdot kt^{-1}$), and Zn (16,510 $g \cdot kt^{-1}$) in the United States than the global averages (Hg (37 $g \cdot kt^{-1}$), Cd (75 $g \cdot kt^{-1}$), Cr (490 $g \cdot kt^{-1}$), Ni (202 $g \cdot kt^{-1}$), Mn (2,685 $g \cdot kt^{-1}$), and Zn (10,754 $g \cdot kt^{-1}$)). Considering their toxicity, high emissions of heavy metals from ISI are of particular concern for public health, especially in countries using EAFs.

3.3 Historical trends of air pollutant emissions and driving forces

The global output of ISI increased significantly from 347 $Mt \cdot year^{-1}$ in 1960 to 595 $Mt \cdot year^{-1}$ in 1970, remained relatively stable at around 700 $Mt \cdot year^{-1}$ between 1970 and 1995, and then began to rise again after 1995 (Figure 3). The stagnation between 1970 and 1995 was primarily due to the oil crisis, changes in the international currency exchange rate, and economic depression in western countries.[20] The rise after 1995 was largely driven by China's production growth.[59]

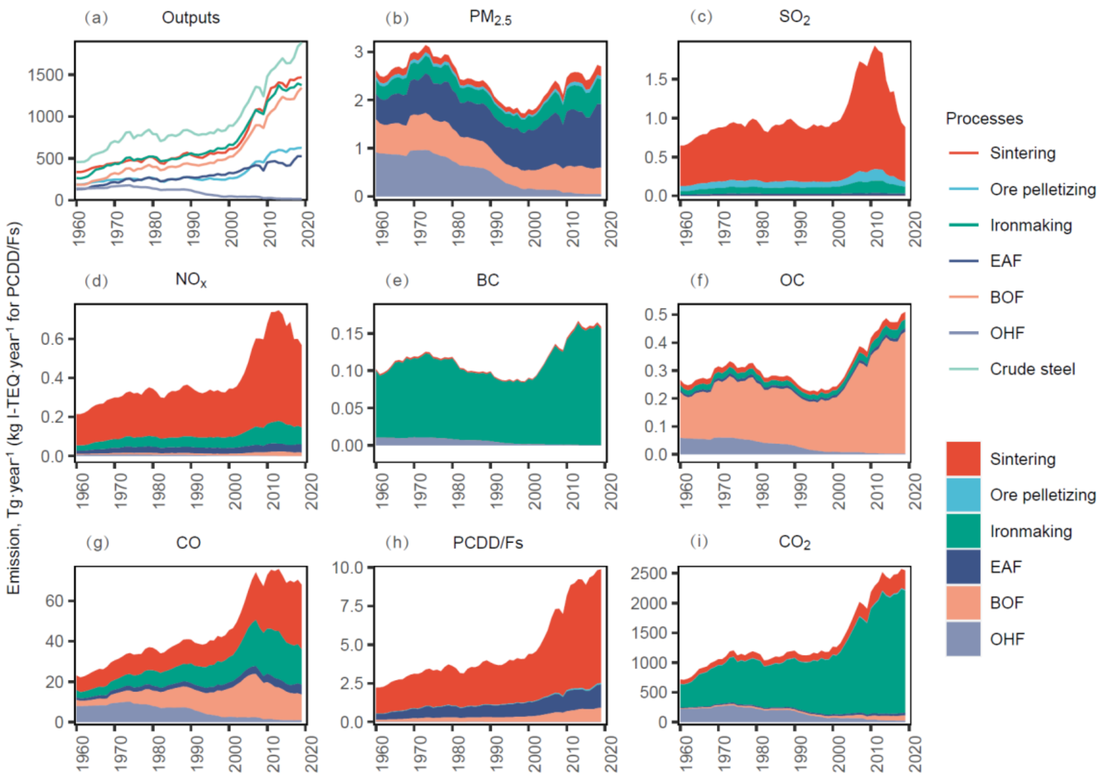

Figure 3. Global trends of the crude steel production output and the emissions of air pollutants and CO_2 between 1960 and 2019. The output of crude steel is the sum of the output from EAF, BOF, and OHF.

Over time, changes in outputs, production technology, and removal efficiency have led to significant variations in ISI emissions. Figures 3 and 4 show the emission trends by process and country category. The $PM_{2.5}$ emission trend exhibits a winding pattern, increasing before 1970 and after 2000, with a decrease in between. The increases in emissions before 1970 and after 2000 were mainly driven by the increases in ISI output, and the decrease in emissions between the 1970s and 1990s was due to a significant decline in OHF production capacity.[36] Most OHFs worldwide were closed by the early 1990s due to their low fuel efficiency and high resource intensity, and were replaced by BOFs.[59] This technology turnover resulted in a long-term decrease in emissions between 1970 and 2000. After 2000, with a substantial increase in steel outputs driven by BOF, China's $PM_{2.5}$ emissions increased rapidly (Figure 4a). However, the installation of end-of-pipe abatement facilities has limited the increase in emissions relative to the increase in steel output. The annual increase rate of steel output was 11.4% between 2000 and 2019 in China, 1.7 times that of $PM_{2.5}$ emissions. A similar decoupling of emissions from production was also observed in other developing countries, where the increase rate of $PM_{2.5}$ emissions (1.2%) was less than half of the increase rate of steel output (2.5%).

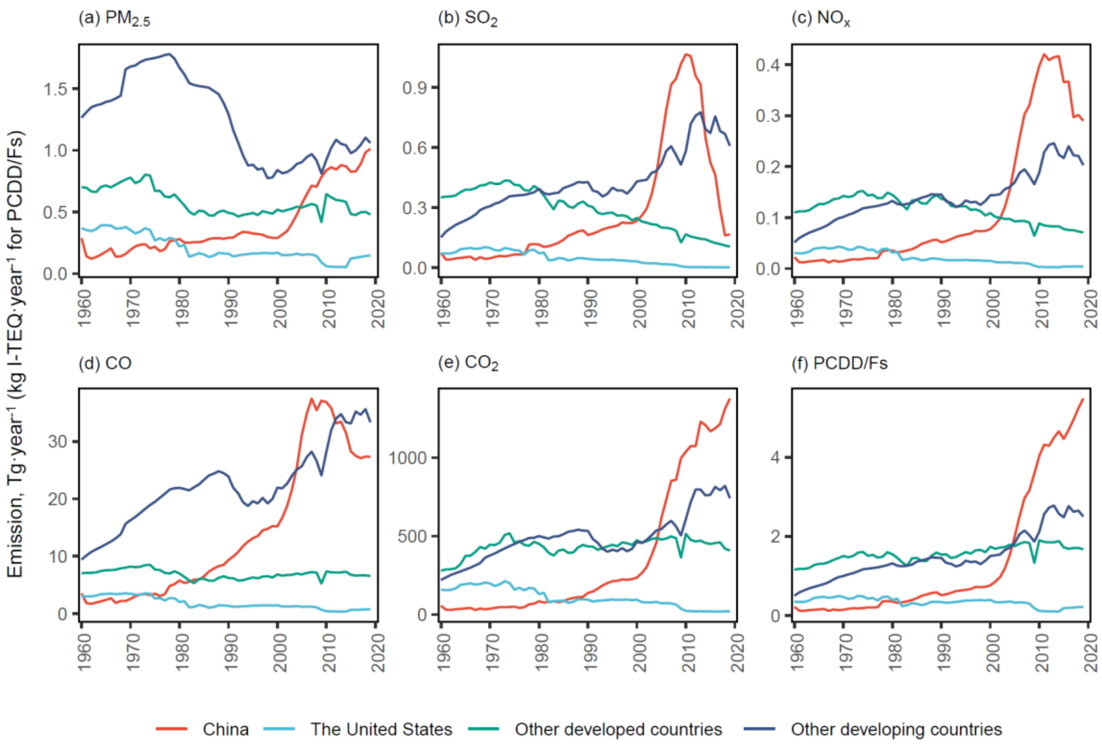

Figure 4. Temporal trends in CO_2 and air pollutants emissions for different country categories during the period 1960–2019.

In contrast to PM, which is mainly emitted during iron and steelmaking processes, most SO_2 and NO_x emissions come from sintering. Before 2000, the emissions of SO_2 and NO_x increased at a low growth rate (1% per year), similar to the growth rate of sintering output (1.5% per year) (Figure 3a, 3c and 3d). After 2000, the rapid growth of sintering output led to a significant increase in emissions (5.5% per year), with China being the main contributor. Since around 2013, end-of-pipe control implemented in China and other "latecomers" has substantially reduced the emission intensities of SO_2 and NO_x.

The global SO_2 emission per ton of iron was cut by 52% (from 1.34 to 0.64 kg/t) between 2013 and 2019, and for NO_x by 24% (from 0.54 to 0.41 kg/t). As a result, the global trends reversed after 2013, decreasing rapidly at annual rates of -9.9% for SO_2 and -3.8% for NO_x (Figures 3c, 3d, 4b and 4c). Developed countries show a gradual decrease in SO_2 and NO_x emissions after 1970 due to stringent controls and improvements in production technology (Figure 4b and 4c).

Generally, $PM_{2.5}$ and SO_2 represent two typical patterns of global emission trends. BC and OC follow the trend of $PM_{2.5}$, while NO_x, CO, PCDD/Fs, and CO_2 follow the trend of SO_2. All pollutants except heavy metals showed rapid increases after 2000 due to the growth of production in China and other emerging countries. Therefore, whether there has been a reversal of the trend in recent years largely depends on how these countries have addressed emission control. For example, the adoption of gas-recycling technology in China has halted the global increase in CO emissions that would otherwise have occurred with growing production (Figures 3g and 4d). In contrast, due to the lack of cost-effective end-of-pipe control measures, the emission intensity of CO_2 is mainly determined by the production process and technology and is relatively stable in the short term. As a result, the growing production has led to a rapid increase in CO_2 emissions (at an annual rate of 3.7% after 2000) (Figure 3i). Given the significant contributions of ISI to global CO_2 emissions (7–10%),[3] the recent rapid increase in CO_2 emissions from ISI has important climate implications. Unlike other pollutants, most heavy metals showed decreasing trends over the study period due to the use of more effective flue gas abatement facilities (see Text S2 and Figures S4 and S5 for details on heavy metals).

We conduct a what-if analysis to demonstrate the impacts of different drivers on global ISI emissions (Text S3). The results depicting $PM_{2.5}$, SO_2, NO_x, and CO_2 emissions are shown in Figure 5, and those for individual country categories are presented in Figure S6 and Text S4. We consider the changes in production process and technology as the structural shift of ISI, and the adoption of abatement devices as end-of-pipe control. In the absence of the structural shift and end-of-pipe control measures, the emissions of

$PM_{2.5}$, SO_2, NO_x and CO_2 from ISI would have reached 19.8, 3.1, 1.3 and 4,492 Tg in 2019 (Figure 5). This implies that the adoption of advanced production technologies and end-of-pipe controls averted emissions of 17.1 Tg $PM_{2.5}$, 2.2 Tg SO_2, 0.7 Tg NO_x, and 1,943 Tg CO_2 in 2019, amounting to 633%, 245%, 129% and 76% of the actual emissions, respectively. The primary driver responsible for CO_2 reduction (1,940 $Tg{\cdot}year^{-1}$) is the structural shift, mainly transitioning from OHF and BOF to EAF. Conversely, end-of-pipe control represents the main driver for $PM_{2.5}$ reduction, accounting for 91% of the overall reduction (15.5 $Tg{\cdot}year^{-1}$). Both drivers have significantly contributed to the reduction of global SO_2 and NO_x emissions, with the structural shift consistently aiding in emissions reduction over time, and end-of-pipe controls assuming an increasingly prominent role in recent years (Figure 5b and 5c).

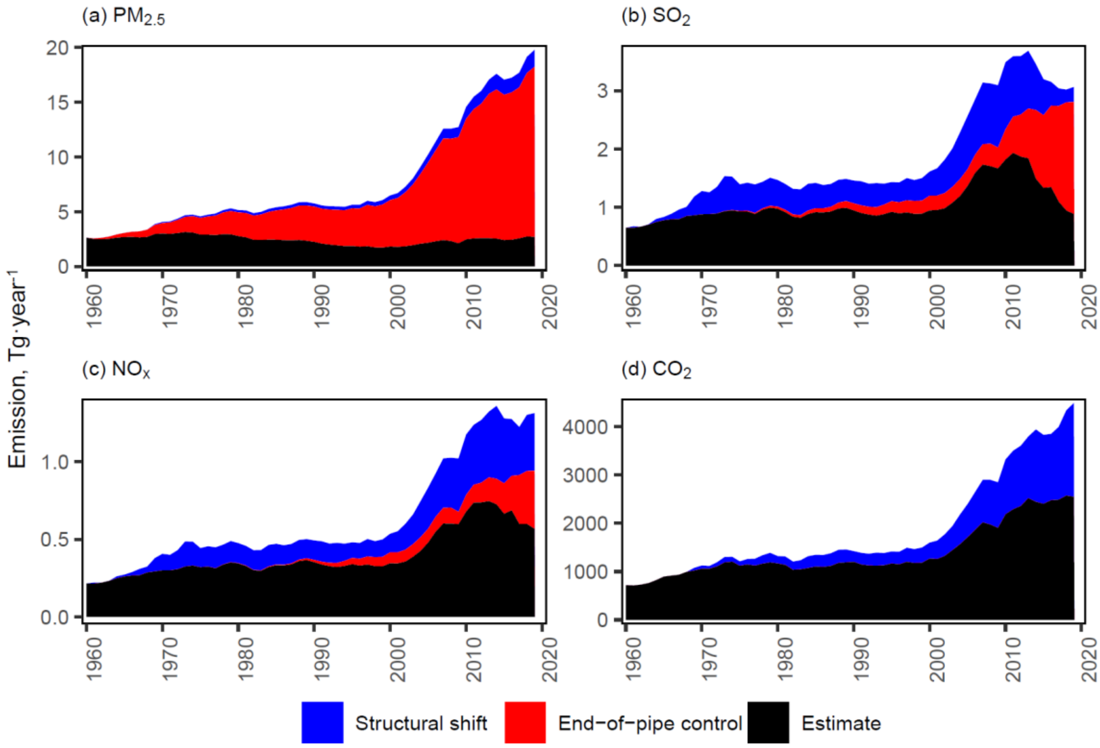

Figure 5. Trends of global emissions from the iron and steel industry under actual and counterfactual scenarios. The black areas illustrate the actual emission trends, while the red areas depict the extent of emission reduction attributed to deployment of end-of-pipe control measures. The blue areas represent the magnitude of emission change resulting from structural shifts, i.e., alterations in production process and technology.

3.4 Future projection

The changing process structure and improved removal efficiency are two main factors that have contributed to the reduction in emissions. With consideration of these two factors, we set up different scenarios to assess future trends up to 2050. The projections of $PM_{2.5}$, SO_2, and CO_2 emissions under different scenarios are shown in Figure 6.

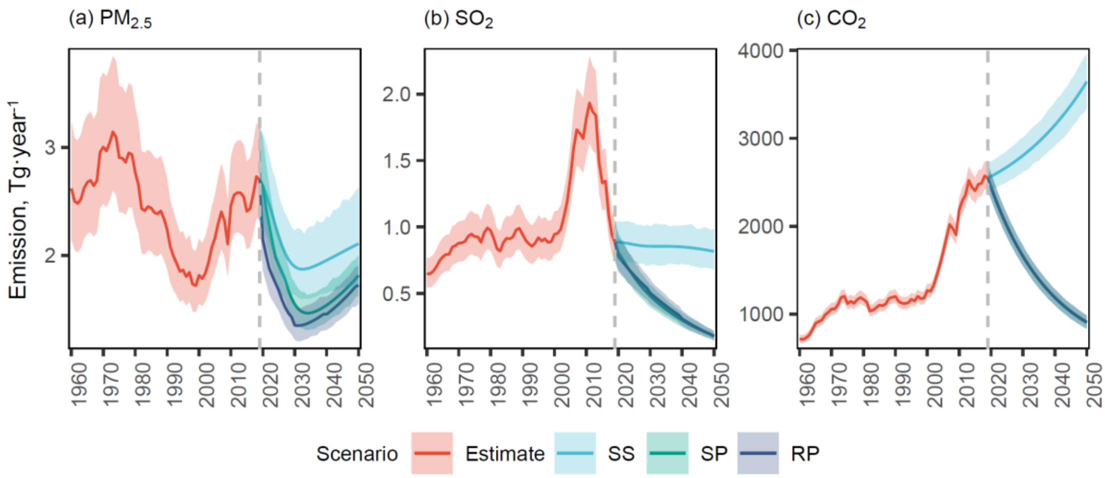

Figure 6. Projections of $PM_{2.5}$, SO_2 and CO_2 emissions under different scenarios.

Before 2030, $PM_{2.5}$ emission from ISI is projected to decrease in all three scenarios (Figure 6a). In April 2019, the Chinese government issued the Opinions on Promoting the Implementation of Ultra Low Emissions in the Iron and Steel Industry, which put forward ultra-low emission limits for various pollutants in the ISI.[60] The projected decrease in the global ISI emission by 2030 is primarily due to a promise of continuing successful implementation of the ultra-low emission transformation in China (Figure S7a).

We estimate that emissions will reach a turning point around 2030 and subsequently rebound due to the inability of abatement measures to counterbalance the demand-driven increase in output, especially in emerging economies. As a result, developing countries (excluding China) are projected to account for 52–54% of global emissions by 2050, compared to 29% in 2019. Driven by stricter environmental protection policies, the decline in emissions before 2030 is expected to be more significant in the SP and RP scenarios compared to the SS scenario. However, regardless of the scenario, an emission rebound is anticipated. It should be noted that these scenarios do not consider technological innovation.

The historical and future trends exhibit several ups and downs in global $PM_{2.5}$ emissions from ISI (Figure 6a). While the upward trends during the periods 1960–1970 and 2000–2020 are consistently driven by growing production, the downward trends are caused by either technology turnover (e.g., 1970–2000) or stringent emission control (e.g., 2020–2030). Currently, feasible production and abatement technologies are not enough to bring down emissions after 2030. Sustaining the future downward trend requires technological innovation and widespread adoption of new technologies by developing countries.

Regarding other pollutants, we find that SO_2 emissions stabilize under the SS scenario but decrease significantly under the SP and RP scenarios. This can be attributed to the enhanced removal efficiencies in developing nations, which possess substantial potential for SO_2 reduction (Figure 6b and S7b). It should be noted that NO_x generally follows a similar trend to SO_2 (Figure S8a), and CO_2 is also projected to decline under the SP and RP scenarios due to the more rapid adoption of EAF and steel recycling technology compared to the SS scenario (Figure 6c). In our scenario analysis, we exclude the impacts of carbon capture, utilization, and storage (CCUS) and other emergent, low-maturity technologies potentially applicable to ISI. As a result, our projected CO_2 emissions may be elevated compared to the IEA's forecasts. For instance, in the SS scenario, our CO_2 projections for 2030 and 2050 are 2.8 Gt and 3.6 Gt, respectively, higher than IEA's Stated Policies Scenario, which predicts 2.8 Gt by 2050. Notably, under the SP and RP scenarios, we anticipate CO_2 emissions to decrease to 1.6 Gt by 2030, aligning with the IEA's Near Zero Carbon Scenario projection of 1.8 Gt.[61] However, our projection of 0.9 Gt CO_2 emissions by 2050 significantly exceeds the IEA's estimate of 0.2 Gt.[61] This suggests that while advancements in steelmaking technology offer significant potential for emission reduction, the long-term priority lies in the implementation of new CCUS technologies. In general, the development and adoption of new production technology and abatement devices, as well as the implementation of strict end-of-pipe controls by China and emerging countries, will contribute to curtailing the upward trajectory of $PM_{2.5}$ and CO_2 emissions while maintaining low levels of other pollutants. This global strategy for ISI is likely to provide significant benefits for both climate and public health.

In this study, we conducted estimations of ISI emissions of CO_2, conventional air pollutants, and various unconventional toxic substances like heavy metals and polychlorinated dibenzodioxins and dibenzofurans. We analyzed emission trends spanning the last six decades and complemented this analysis with projections extending until 2050. $PM_{2.5}$ emissions demonstrated a sustained decline between 1970 and 2000, due mainly to the adoption of advanced production technologies. NO_x and SO_2, on the other hand, have only recently started to decline as a result of effective emission controls in major emitters such as China, which are anticipated to continue in the near future. Decomposition analysis showed that the implementation of end-of-pipe abatement technologies is instrumental in curbing $PM_{2.5}$ emissions in the current stage, while modifications in process structures are key to reducing CO_2 emissions. The spatial distribution of emissions within ISI has witnessed significant changes over time, with rapid growth observed in China's ISI sector. Our predictions suggest a shifting emission focus within ISI toward emerging developing countries in the future. During this transition, the transformation of steelmaking production structures and the adoption of abatement measures will necessitate substantial innovation to fit climate and air quality goals.

It is important to acknowledge that the current research possesses certain limitations that warrant further exploration in future studies. Although we have distinguished differences in removal efficiency across countries within various categories, significant variations also exist at the plant level within the same country due to factors such as differences in construction years, production technologies, and regional policies. Addressing these variances would require more detailed and accurate foundational information. Additionally, in the context of future emission projections, more comprehensive parameter settings may be needed to account for the influence of factors like population, economy, social development, and climate goals. These factors are intricately linked to steel production and the implementation of environmental policies, making them pivotal for predicting future emission scenarios.

Supporting Information contains supplementary tables and figures with additional information on the activity data, emission factors adopted in this study, parameterization for technology splits, comparison with previous inventories, the emissions by country in 2019, heavy metals emissions trends, and projections under different scenarios. Supplementary Data provides process-specific activity data spanning the years 1960 through 2019 at five-year intervals, with annual data provided for 2015–2019.

Acknowledgements

This research is supported by the National Natural Science Foundation of China (42192511), the Shenzhen Key Laboratory of Precision Measurement and Early Warning Technology for Urban Environmental Health Risks (ZDSYS20220606100604008), Shenzhen Science and Technology Program (JCYJ20220818100611024), the National Natural Science Foundation of China (41991312, 41821005, 41922057, and 41830641), Department of Science and Technology of Guangdong Province (2021B1212050024), Department of Education of Guangdong Province (2021KCXTD004), Energy Foundation (G-2111-33575), and Center for Computational Science and Engineering at Southern University of Science and Technology.

Reference

(1) Gao, C.; Gao, W.; Song, K.; Na, H.; Tian, F.; Zhang, S. Spatial and Temporal Dynamics of Air-Pollutant Emission Inventory of Steel Industry in China: A Bottom-up Approach. *Resources, Conservation and Recycling* **2019**, *143*, 184–200. https://doi.org/10.1016/j.resconrec.2018.12.032.

(2) Ren, L.; Zhou, S.; Peng, T.; Ou, X. A Review of CO2 Emissions Reduction Technologies and Low-Carbon Development in the Iron and Steel Industry Focusing on China. *Renewable and Sustainable Energy Reviews* **2021**, *143*, 110846. https://doi.org/10.1016/j.rser.2021.110846.

(3) IEA, Iron and Steel Technology Roadmap; Paris, 2020. https://www.iea.org/reports/iron-and-steel-technology-roadmap.

(4) Kim, J.; Sovacool, B. K.; Bazilian, M.; Griffiths, S.; Lee, J.; Yang, M.; Lee, J. Decarbonizing the Iron and Steel Industry: A Systematic Review of Sociotechnical Systems, Technological Innovations, and Policy Options. *Energy Research & Social Science* **2022**, *89*, 102565. https://doi.org/10.1016/j.erss.2022.102565.

(5) Quader, M. A.; Ahmed, S.; Ghazilla, R. A. R.; Ahmed, S.; Dahari, M. A Comprehensive Review on Energy Efficient CO2 Breakthrough Technologies for Sustainable Green Iron and Steel Manufacturing. *Renewable and Sustainable Energy Reviews* **2015**, *50*, 594–614. https://doi.org/10.1016/j.rser.2015.05.026.

(6) Wang, K.; Tian, H.; Hua, S.; Zhu, C.; Gao, J.; Xue, Y.; Hao, J.; Wang, Y.; Zhou, J. A Comprehensive Emission Inventory of Multiple Air Pollutants from Iron and Steel Industry in China: Temporal Trends and Spatial Variation Characteristics. *Science of The Total Environment* **2016**, *559*, 7–14. https://doi.org/10.1016/j.scitotenv.2016.03.125.

(7) Wang, H.; Zhang, P. Emission Characteristics of PM, Heavy Metals, and Dioxins in Flue Gases from Sintering Machines with Wet and Semi-Dry Flue Gas Desulfurization Systems. *Environ. Sci. Pollut. Res.* **2021**, *28* (34), 46089–46099.

https://doi.org/10.1007/s11356-020-11500-w.

(8) Wang, Y.; Wen, Z.; Cao, X.; Zheng, Z.; Xu, J. Environmental Efficiency Evaluation of China's Iron and Steel Industry: A Process-Level Data Envelopment Analysis. *Science of The Total Environment* **2020**, *707*, 135903. https://doi.org/10.1016/j.scitotenv.2019.135903.

(9) Tang, L.; Xue, X.; Jia, M.; Jing, H.; Wang, T.; Zhen, R.; Huang, M.; Tian, J.; Guo, J.; Li, L.; Bo, X.; Wang, S. Iron and Steel Industry Emissions and Contribution to the Air Quality in China. *Atmospheric Environment* **2020**, *237*, 117668. https://doi.org/10.1016/j.atmosenv.2020.117668.

(10) Li, M.; Liu, H.; Geng, G.; Hong, C.; Liu, F.; Song, Y.; Tong, D.; Zheng, B.; Cui, H.; Man, H.; Zhang, Q.; He, K. Anthropogenic Emission Inventories in China: A Review. *National Science Review* **2017**, *4* (6), 834–866. https://doi.org/10.1093/nsr/nwx150.

(11) Xu, W.; Shao, M.; Yang, Y.; Liu, R.; Wu, Y.; Zhu, T. Mercury Emission from Sintering Process in the Iron and Steel Industry of China. *Fuel Processing Technology* **2017**, *159*, 340–344. https://doi.org/10.1016/j.fuproc.2017.01.033.

(12) Zhang, H.; Sun, W.; Li, W.; Wang, Y. Physical and Chemical Characterization of Fugitive Particulate Matter Emissions of the Iron and Steel Industry. *Atmospheric Pollution Research* **2022**, *13* (1), 101272. https://doi.org/10.1016/j.apr.2021.101272.

(13) Buekens, A.; Stieglitz, L.; Hell, K.; Huang, H.; Segers, P. Dioxins from Thermal and Metallurgical Processes: Recent Studies for the Iron and Steel Industry. *Chemosphere* **2001**, *42* (5–7), 729–735. https://doi.org/10.1016/S0045-6535(00)00247-2.

(14) Jager, J. PCDD/F and PCB Emission from Steel Producing, Processing and Reclamation Plants with Varying Input. *Toxicological & Environmental Chemistry* **1993**, *40* (1–4), 201–211. https://doi.org/10.1080/02772249309357944.

(15) Huang, Y.; Chen, Y.; Li, Y.; Zhou, L.; Zhang, S.; Wang, J.; Du, W.; Yang, J.; Chen, L.; Meng, W.; Tao, S.; Liu, M. Atmospheric Emissions of PCDDs and PCDFs in China from 1960 to 2014. *Journal of Hazardous Materials* **2022**, *424*, 127320. https://doi.org/10.1016/j.jhazmat.2021.127320.

(16) Dong, M. Investigation on the PCDD/Fs Distribution of Quenched off-Gas from Electric Arc Furnace. *Chemosphere* **2021**, *272*, 129932. https://doi.org/10.1016/j.chemosphere.2021.129932.

(17) Salian, K.; Strezov, V.; Evans, T. J.; Taylor, M.; Nelson, P. F. Application of National Pollutant Inventories for Monitoring Trends on Dioxin Emissions from Stationary Industrial Sources in Australia, Canada and European Union. *PLoS ONE* **2019**, *14* (10), e0224328. https://doi.org/10.1371/journal.pone.0224328.

(18) Jia, J.; Cheng, S.; Yao, S.; Xu, T.; Zhang, T.; Ma, Y.; Wang, H.; Duan, W. Emission Characteristics and Chemical Components of Size-Segregated Particulate Matter in Iron and Steel Industry. *Atmospheric Environment* **2018**, *182*, 115–127. https://doi.org/10.1016/j.atmosenv.2018.03.051.

(19) Wang, X.; Lei, Y.; Yan, L.; Liu, T.; Zhang, Q.; He, K. A Unit-Based Emission Inventory of SO2, NOx and PM for the Chinese Iron and Steel Industry from 2010 to 2015. *Science of The Total Environment* **2019**, *676*, 18–30. https://doi.org/10.1016/j.scitotenv.2019.04.241.

(20) World Steel in Figures 2022, https://worldsteel.org/wp-content/uploads/World-Steel-in-Figures-2022-CN.pdf?x65430 (accessed 2022-09-13).

(21) Hasanbeigi, A., Bhadbhade, N., Ghosh, A. 2022. Air Pollution from Global Steel Industry - An International Benchmarking of Criteria Air Pollutants Intensities. Global Efficiency Intelligence. Florida, United States.

(22) Protopopov, E. V.; Feyler, S. V. Analysis of Current State and Prospects of Steel Production Development. *IOP Conf. Ser.: Mater. Sci. Eng.* **2016**, *150*, 012001. https://doi.org/10.1088/1757-899X/150/1/012001.

(23) Wang, X.; Yan, L.; Lei, Y.; He, K.; He, J. Estimation of primary particulate emissions from iron and steel industry in China. Acta Scientiae Circumstantiae. 2016, 36 (8):3033-3039.

(24) Wu, X.; Zhao, L.; Zhang, Y.; Zheng, C.; Gao, X.; Cen, K. Primary Air Pollutant Emissions and Future Prediction of Iron and Steel Industry in China. *Aerosol Air Qual. Res.* **2015**, *15* (4), 1422–1432. https://doi.org/10.4209/aaqr.2015.01.0029.

(25) Lei, Y.; Zhang, Q.; He, K.; Streets, D. G. Primary Anthropogenic Aerosol Emission Trends for China, 1990-2005. *Atmospheric Chemistry and Physics* **2011**, *11*.

(26) *The Latecomer Advantages and Disadvantages: A New Structural Economics Perspective*. https://www.nse.pku.edu.cn/xzyj/gzlw/gzlw2/244115.htm (accessed 2022-09-09).

(27) Zhu, T.; Wang, X.; Yu, Y.; Li, C.; Yao, Q.; Li, Y. Multi-Process and Multi-Pollutant Control Technology for Ultra-Low Emissions in the Iron and Steel Industry. *Journal of Environmental Sciences* **2022**, S1001074222000572. https://doi.org/10.1016/j.jes.2022.01.044.

(28) Yi, X.; Wen-bo, Z.; Wei, S.; Wei, W.; Xiu-juan, Z.; Jing-xiao, Y. Research of Ultra-Low Emission Technologies of the Iron and Steel Industry in China. *Chinese Journal of Engineering*, 2021, *43*, 1.

(29) Liu, J.; Wang, S.; Yi, H.; Tang, X.; Li, Z.; Yu, Q.; Zhao, S.; Gao, F.; Zhou, Y.; Wang, Y. Air Pollutant Emission and Reduction Potentials from the Sintering Process of the Iron and Steel Industry in China in 2017. *Environmental Pollution* **2022**, *307*, 119512. https://doi.org/10.1016/j.envpol.2022.119512.

(30) Opinions on Promoting the Implementation of Ultra low Emission in the Iron and Steel Industry. https://www.mee.gov.cn/xxgk2018/xxgk/xxgk03/201904/t20190429_701463.html (accessed 2022-09-09).

(31) Mousa, E.; Wang, C.; Riesbeck, J.; Larsson, M. Biomass Applications in Iron and

Steel Industry: An Overview of Challenges and Opportunities. *Renew. Sust. Energ. Rev.* **2016**, *65*, 1247–1266. https://doi.org/10.1016/j.rser.2016.07.061.

(32) Na, H.; Sun, J.; Qiu, Z.; He, J.; Yuan, Y.; Yan, T.; Du, T. A Novel Evaluation Method for Energy Efficiency of Process Industry — A Case Study of Typical Iron and Steel Manufacturing Process. *Energy* **2021**, *233*, 121081. https://doi.org/10.1016/j.energy.2021.121081.

(33) He, K.; Wang, L.; Li, X. Review of the Energy Consumption and Production Structure of China's Steel Industry: Current Situation and Future Development. *Metals* **2020**, *10* (3), 302. https://doi.org/10.3390/met10030302.

(34) Tian, B.; Wei, G.; Li, X.; Zhu, R.; Bai, H.; Tian, W.; Dong, K. Effect of Hot Metal Charging on Economic and Environmental Indices of Electric Arc Furnace Steelmaking in China. *Journal of Cleaner Production* **2022**, *379*, 134597. https://doi.org/10.1016/j.jclepro.2022.134597.

(35) Wang, C.; Ryman, C.; Dahl, J. Potential CO2 Emission Reduction for BF–BOF Steelmaking Based on Optimised Use of Ferrous Burden Materials. *International Journal of Greenhouse Gas Control* **2009**, *3* (1), 29–38. https://doi.org/10.1016/j.ijggc.2008.06.005.

(36) *Steel statistical yearbook*. worldsteel.org. https://worldsteel.org/steel-topics/statistics/steel-statistical-yearbook/ (accessed 2022-08-25).

(37) Wang, R.; Tao, S.; Ciais, P.; Shen, H. Z.; Huang, Y.; Chen, H.; Shen, G. F.; Wang, B.; Li, W.; Zhang, Y. Y.; Lu, Y.; Zhu, D.; Chen, Y. C.; Liu, X. P.; Wang, W. T.; Wang, X. L.; Liu, W. X.; Li, B. G.; Piao, S. L. High-Resolution Mapping of Combustion Processes and Implications for CO2 Emissions. *Atmos. Chem. Phys.* **2013**, *13* (10), 5189–5203. https://doi.org/10.5194/acp-13-5189-2013.

(38) Mourão, J. M.; Patel, N.; Huerta, M.; Cameron, I.; Pereira, R. COMPARISON OF SINTER AND PELLET USAGE IN AN INTEGRATED STEEL PLANT. 43o Seminário de Redução de Minério de Ferro e Matérias-Primas e o 14o Simpósio Brasileiro de Minério de Ferro 2013, 43 (43), 462–472. https://doi.org/10.5151/2594-357X-23845.

(39) Huang, Y.; Shen, H.; Chen, H.; Wang, R.; Zhang, Y.; Su, S.; Chen, Y.; Lin, N.; Zhuo, S.; Zhong, Q.; Wang, X.; Liu, J.; Li, B.; Liu, W.; Tao, S. Quantification of Global Primary Emissions of PM2.5, PM10, and TSP from Combustion and Industrial Process Sources. *Environ. Sci. Technol.* **2014**, *48* (23), 13834–13843. https://doi.org/10.1021/es503696k.

(40) Zhong, Q.; Huang, Y.; Shen, H.; Chen, Y.; Chen, H.; Huang, T.; Zeng, E. Y.; Tao, S. Global Estimates of Carbon Monoxide Emissions from 1960 to 2013. *Environ Sci Pollut Res* **2017**, *24* (1), 864–873. https://doi.org/10.1007/s11356-016-7896-2.

(41) Bond, T. C.; Bhardwaj, E.; Dong, R.; Jogani, R.; Jung, S.; Roden, C.; Streets, D. G.; Trautmann, N. M. Historical Emissions of Black and Organic Carbon Aerosol from Energy-Related Combustion, 1850-2000: HISTORICAL BC/OC EMISSIONS. *Global Biogeochem. Cycles* **2007**, *21* (2), n/a-n/a. https://doi.org/10.1029/2006GB002840.

(42) Shen, H.; Huang, Y.; Wang, R.; Zhu, D.; Li, W.; Shen, G.; Wang, B.; Zhang, Y.; Chen, Y.; Lu, Y.; Chen, H.; Li, T.; Sun, K.; Li, B.; Liu, W.; Liu, J.; Tao, S. Global Atmospheric Emissions of Polycyclic Aromatic Hydrocarbons from 1960 to 2008 and Future Predictions. *Environ. Sci. Technol.* **2013**, *47* (12), 6415–6424. https://doi.org/10.1021/es400857z.

(43) Liu, H.; Wang, C.; Zhang, M.; Wang, S. Evaluating the Effects of Air Pollution Control Policies in China Using a Difference-in-Differences Approach. *Science of The Total Environment* **2022**, *845*, 157333. https://doi.org/10.1016/j.scitotenv.2022.157333.

(44) Zhao, Y.; Nielsen, C. P.; McElroy, M. B.; Zhang, L.; Zhang, J. CO Emissions in China: Uncertainties and Implications of Improved Energy Efficiency and Emission Control. *Atmospheric Environment* **2012**, *49*, 103–113. https://doi.org/10.1016/j.atmosenv.2011.12.015.

(45) Streets, D. G.; Zhang, Q.; Wang, L.; He, K.; Hao, J.; Wu, Y.; Tang, Y.; Carmichael, G. R. Revisiting China's CO Emissions after the Transport and Chemical Evolution

over the Pacific (TRACE-P) Mission: Synthesis of Inventories, Atmospheric Modeling, and Observations. *Journal of Geophysical Research: Atmospheres* **2006**, *111* (D14). https://doi.org/10.1029/2006JD007118.

(46) *Control Techniques for Carbon Monoxide Emissions from Stationary Sources*; United States, Ed.; Its Publication; For sale by the Supt. of Docs., U.S. Govt. Print. Off: Washington, 1970.

(47) Shen, H.; Tao, S.; Chen, Y.; Ciais, P.; Güneralp, B.; Ru, M.; Zhong, Q.; Yun, X.; Zhu, X.; Huang, T.; Tao, W.; Chen, Y.; Li, B.; Wang, X.; Liu, W.; Liu, J.; Zhao, S. Urbanization-Induced Population Migration Has Reduced Ambient PM2.5 Concentrations in China. *Science Advances 3* (7), e1700300. https://doi.org/10.1126/sciadv.1700300.

(48) Chen, Y.; Wang, R.; Shen, H.; Li, W.; Chen, H.; Huang, Y.; Zhang, Y.; Chen, Y.; Su, S.; Lin, N.; Liu, J.; Li, B.; Wang, X.; Liu, W.; Coveney, R. M.; Tao, S. Global Mercury Emissions from Combustion in Light of International Fuel Trading. *Environ. Sci. Technol.* **2014**, *48* (3), 1727–1735. https://doi.org/10.1021/es404110f.

(49) Huang, T.; Zhu, X.; Zhong, Q.; Yun, X.; Meng, W.; Li, B.; Ma, J.; Zeng, E. Y.; Tao, S. Spatial and Temporal Trends in Global Emissions of Nitrogen Oxides from 1960 to 2014. *Environ. Sci. Technol.* **2017**, *51* (14), 7992–8000. https://doi.org/10.1021/acs.est.7b02235.

(50) Zhou, X.-H. CONFIDENCE INTERVALS FOR THE LOG-NORMAL MEAN. *STAT. MED.* **1997**, *16*, 8.

(51) *EDGAR - The Emissions Database for Global Atmospheric Research*. https://edgar.jrc.ec.europa.eu/index.php/dataset_ap61 (accessed 2022-09-13).

(52) Hoesly, R. M.; Smith, S. J.; Feng, L.; Klimont, Z.; Janssens-Maenhout, G.; Pitkanen, T.; Seibert, J. J.; Vu, L.; Andres, R. J.; Bolt, R. M.; Bond, T. C.; Dawidowski, L.; Kholod, N.; Kurokawa, J.; Li, M.; Liu, L.; Lu, Z.; Moura, M. C. P.; O'Rourke, P. R.; Zhang, Q. Historical (1750–2014) Anthropogenic Emissions

of Reactive Gases and Aerosols from the Community Emissions Data System (CEDS). *Geosci. Model Dev.* **2018**, *11* (1), 369–408. https://doi.org/10.5194/gmd-11-369-2018.

(53) McDuffie, E. E.; Smith, S. J.; O'Rourke, P.; Tibrewal, K.; Venkataraman, C.; Marais, E. A.; Zheng, B.; Crippa, M.; Brauer, M.; Martin, R. V. A Global Anthropogenic Emission Inventory of Atmospheric Pollutants from Sector- and Fuel-Specific Sources (1970–2017): An Application of the Community Emissions Data System (CEDS). *Earth Syst. Sci. Data* **2020**, *12* (4), 3413–3442. https://doi.org/10.5194/essd-12-3413-2020.

(54) Cui, L.; Liu, M.; Yuan, X.; Wang, Q.; Ma, Q.; Wang, P.; Hong, J.; Liu, H. Environmental and Economic Impact Assessment of Three Sintering Flue Gas Treatment Technologies in the Iron and Steel Industry. *Journal of Cleaner Production* **2021**, *311*, 127703. https://doi.org/10.1016/j.jclepro.2021.127703.

(55) Wang, S.; Liu, J.; Yi, H.; Tang, X.; Yu, Q.; Zhao, S.; Gao, F.; Zhou, Y.; Zhong, T.; Wang, Y. Trends in Air Pollutant Emissions from the Sintering Process of the Iron and Steel Industry in the Fenwei Plain and Surrounding Regions in China, 2014–2017. *Chemosphere* **2022**, *291*, 132917. https://doi.org/10.1016/j.chemosphere.2021.132917.

(56) Lau, L. L.; Strezov, V.; Gonçalves, M. V. B.; Bagatini, M. C. Trace Elements Emission in Iron Ore Sintering: A Review. *Environmental Advances* **2021**, *6*, 100123. https://doi.org/10.1016/j.envadv.2021.100123.

(57) Sofili, T. Characterization of Steel Mill Electric-Arc Furnace Dust. *Journal of Hazardous Materials* **2004**, *109* (1–3), 59–70. https://doi.org/10.1016/j.jhazmat.2004.02.032.

(58) Guézennec, A.-G.; Huber, J.-C.; Patisson, F.; Sessiecq, P.; Birat, J.-P.; Ablitzer, D. Dust Formation in Electric Arc Furnace: Birth of the Particles. *Powder Technology* **2005**, *157* (1–3), 2–11. https://doi.org/10.1016/j.powtec.2005.05.006.

(59) Yellishetty, M.; Ranjith, P. G.; Tharumarajah, A. Iron Ore and Steel Production Trends and Material Flows in the World: Is This Really Sustainable? *Resources, Conservation and Recycling* **2010**, *54* (12), 1084–1094. https://doi.org/10.1016/j.resconrec.2010.03.003.

(60) Opinions on Promoting the Implementation of Ultra Low Emission in the Iron and Steel Industry. https://www.mee.gov.cn/xxgk2018/xxgk/xxgk15/201905/t20190505_701878.html (accessed 2022-11-15).

(61) IEA. Net Zero by 2050; Paris, 2021. https://www.iea.org/reports/net-zero-by-2050.